

Contents lists available at ScienceDirect

Physics Letters A

www.elsevier.com/locate/pla



Spatial bandwidth enlargement and field enhancement of shear horizontal waves in finite graded piezoelectric layered media



Yanlong Xu

Division of Computer, Electrical and Mathematical Sciences and Engineering, King Abdullah University of Science and Technology (KAUST), Thuwal 23955-6900, Saudi Arabia

ARTICLE INFO

Article history: Received 24 December 2014 Received in revised form 5 April 2015 Accepted 6 April 2015 Available online 9 April 2015 Communicated by R. Wu

Keywords: Shear horizontal wave Piezoelectric layered media Band gap Bandwidth enlargement

ABSTRACT

Shear horizontal (SH) wave propagation in finite graded piezoelectric layered media is investigated by transfer matrix method. Different from the previous studies on SH wave propagation in completely periodic layered media, calculations on band structure and transmission in this paper show that the graded layered media possess very large band gaps. Harmonic wave simulation by finite element method (FEM) confirms that the reason of bandwidth enlargement is that waves within the band gap ranges are spatially enhanced and stopped by the corresponding graded units. The study suggests that the graded structure possesses the property of manipulating elastic waves spatially, which shows potential applications in strengthening energy trapping and harvesting.

© 2015 Elsevier B.V. All rights reserved.

1. Introduction

Shear horizontal (SH) wave propagation in layered media has attracted a lot of attention [1–10] in several decades due to its theoretical significance and engineering application. In particular, this wave propagation in infinite periodic layered media [3,5,8,11-14] has been focused on by many researchers in recent years, because of its band gap property, which can be used as new acoustic devices like filters and transducers. Among these works, complicated situations have been considered to study influences of piezoelectricity [13,14], piezomagnetism [11], imperfect interface [12], incident angle [4], disorder [3], and functionally graded material [5] on the band gap property. In this paper, different from the previous studies which are based on the infinite completely periodic cases with emphasis placed on the effect factors of band gap, the finite graded piezoelectric layered media are considered. Here, piezoelectricity is included in view of the fact that the structure may show potential applications in energy absorption and energy harvesting.

The work is triggered by the recent studies of rainbow trapping on electromagnetic and acoustic wave propagation in graded or chirped gratings. Rainbow trapping means that the broadband incident waves will be enhanced and stopped at different spatial positions due to the slow wave effect and finally reflected at the incident side after a certain "trapping time". Originally, this is mainly shown for the electromagnetic surface wave [15] which shows very flat dispersion relation, and later extended to

the acoustic surface wave [16]. The dispersion relation is flat when wave vector approaches the Brillouin boundary, therefore, the incident wave can be slowed, enhanced, and trapped within a certain time [17]. Then, the electromagnetic bulk wave propagation in the one-dimensional chirped photonic crystals [18] and acoustic bulk wave propagation in the graded sonic crystals [19] are also studied to show rainbow trapping phenomenon. In these works only one flat-like band of the dispersion curves is considered to get the enhanced wave fronts. In this paper, all the bands of the dispersion curves in a considered frequency range are considered for the elastic wave with rainbow trapping phenomenon extended to the certain bands. Very large bandwidth and spatially enhanced wave fronts are got for the SH wave propagation through the graded layered media.

The paper is organized as follows. The designed layered model and transfer matrix method computing band structure and transmission are firstly introduced to describe the problem. Then, numerical results on band structure, transmission, and harmonic wave field of incident Gaussian beam computed by finite element method (FEM) are given to show the spatial bandwidth enlargement and wave field enhancement due to the graded characteristic possessed by the layered media. Finally, conclusions are summarized.

2. Model and transfer matrix method

The schematic of the graded layered media is drawn in Fig. 1. The graded units are formed by sublayer 1 with identical thickness

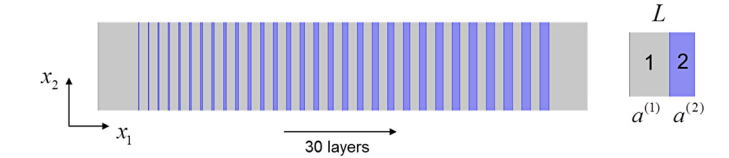


Fig. 1. The schematic of the graded piezoelectric layered media. The thickness-graded sublayer 2 is regularly inserted into medium 1 with an identical thickness interval. L is the thickness of the graded units formed by sublayer 1 with identical thickness $a^{(1)}$ and sublayer 2 with graded thickness $a^{(2)}$. $a^{(2)}$ is linearly increased from 0 to $a^{(1)}$ by 30 layers.

 $a^{(1)}$ and sublayer 2 with graded thickness $a^{(2)}$. $a^{(2)}$ is linearly increased from 0 to $a^{(1)}$ by 30 layers. The maximum thickness of the graded unit is $2a^{(1)}$. Sublayers 1 and 2 both belong to piezoelectric material with material constants shown in Table 1.

When an obliquely incident harmonic wave propagates in a transversely isotropic piezoelectric material with the wave vector located in the plane perpendicular to the material polarization direction, the SH or out of plane wave equation is decoupled from the plane strain or in-plane wave equation. With the quasi-static approximation adopted for the electric field, the SH wave propagation in piezoelectric medium meets the following equation

$$\bar{c}_{44}(u_{3,11} + u_{3,22}) = \rho \ddot{u}_3
\phi_{,11} + \phi_{,22} = \frac{e_{15}}{\varepsilon_{11}} (u_{3,11} + u_{3,22})$$
(1)

where u_3 is the transverse displacement in the x_3 direction, ϕ the electric potential, ρ the mass density, c_{44} the elastic constant, ε_{11} the dielectric constant, e_{15} the piezoelectric coefficient, and $\bar{c}_{44} = c_{44} + e_{15}^2/\varepsilon_{11}$. The general solution of Eq. (1) can be assumed as

$$u_3(x_1, x_2, t) = u(x_1)e^{i(k_2x_2 - \omega t)}$$

$$\phi(x_1, x_2, t) = \phi(x_1)e^{i(k_2x_2 - \omega t)}$$
(2)

where ω is the circular frequency, $i = \sqrt{-1}$, and k_2 equal to $k \sin(\theta_0)$ with k the wave vector and θ_0 the incident angle. Substituting Eq. (2) into Eq. (1), $u(x_1)$ and $\phi(x_1)$ can be solved as follows

$$u(x_1) = Ae^{iqx_1} + Be^{-iqx_1}$$

$$\phi(x_1) = Ce^{k_2x_1} + De^{-k_2x_1} + \frac{e_{15}}{\varepsilon_{11}} (Ae^{iqx_1} + Be^{-iqx_1})$$
(3)

where $q=\sqrt{\omega^2\rho/\bar{c}_{44}-k_2^2}$ and the coefficients C and D represent the electric potential surface wave. For small incident angle, the coefficients C and D can be taken zero to simplify the calculation, which is called non-surface wave approximation in Refs. [2, 10]. Recalling the constitutive relations: $T_{31}=c_{44}u_{3,1}+e_{15}\phi_{,1}$ and $D_1=e_{15}u_{3,1}-\varepsilon_{11}\phi_{,1}$, the stress T_{31} and electric displacement D_1 can be expressed as

$$T_{31} = iq\bar{c}_{44} (Ae^{iqx_1} + Be^{-iqx_1}) + k_2e_{15} (Ce^{k_2x_1} - De^{-k_2x_1})$$

$$D_1 = -k_2\varepsilon_{11} (Ce^{k_2x_1} - De^{-k_2x_1})$$
(4)

From Eq. (4), one can see that the electric displacement D_1 only depends on the electric potential surface wave.

For the layered media, the physical quantities u_3 , ϕ , T_{31} and D_1 on the interface of each layer can be organized as a state vector:

 $\mathbf{v} = \{u_3, T_{31}, \phi, D_1\}^T$. The state vector on the left boundary \mathbf{v}_L and that on the right boundary \mathbf{v}_R of the i-th graded unit can be connected by a transfer matrix \mathbf{T}_i , according to the general solutions of Eqs. (3) and (4). The transfer matrix is a function of the frequency and sublayers' thickness. For sublayer 1, one has $\mathbf{v}_R^{(1)} = \mathbf{T}_i^{(1)} \mathbf{v}_L^{(1)}$, and sublayer 2, $\mathbf{v}_R^{(2)} = \mathbf{T}_i^{(2)} \mathbf{v}_L^{(2)}$. Considering that the interfaces between sublayer 1 and sublayer 2 are perfectly bonded, one has the continuity condition $\mathbf{v}_R^{(1)} = \mathbf{v}_L^{(2)}$. So the relationship of the state vector of the left boundary in sublayer 1 and that of the right boundary in sublayer 2 can be written as

$$\mathbf{v}_{R}^{(2)} = \mathbf{T}_{i}^{(2)} \mathbf{v}_{L}^{(2)} = \mathbf{T}_{i}^{(2)} \mathbf{v}_{R}^{(1)} = \mathbf{T}_{i}^{(2)} \mathbf{T}_{i}^{(1)} \mathbf{v}_{L}^{(1)} = \mathbf{T}_{i} \mathbf{v}_{L}^{(1)}$$
(5)

Here, the dimensions of the transfer matrix are 4×4 . When the non-surface wave approximation is adopted, the dimensions of the transfer matrix are 2×2 with the state vector \mathbf{v} degenerating into $\{u_3, T_{31}\}^T$. The transfer matrices for the sublayer with and without electric potential surface wave considered are given in Appendix A.

To compute band structure of the corresponding infinite completely periodic layered media stacked by each graded unit like the i-th unit, a phase relation related to the wave number defining boundary conditions between the adjacent units can be applied to the state vectors according to Bloch theorem: $\mathbf{v}_{\mathrm{R}}^{(2)} = e^{iKL_i}\mathbf{v}_{\mathrm{L}}^{(1)}$. K is the Bloch wave vector taken values from the range $(0,\pi/L_i)$. With Eq. (5), one can get $(\mathbf{T}_i - e^{iKL_i}\mathbf{I})\mathbf{v}_{\mathrm{L}}^{(1)} = 0$. Band structure can be computed making the coefficient determinant of the equation equal to zero, i.e.

$$|\mathbf{T}_i - e^{iKL_i}\mathbf{I}| = 0 \tag{6}$$

For transmission calculation, the transfer matrix method will be numerically unstable inherently when the dimensions of the transfer matrix are large. There are many other matrix methods [6,7,9] proposed overcoming this disadvantage to compute the transmission of the layered media. For simplicity and consistency, a non-surface wave approximation will be adopted here to make the transmission calculation easier, numerically stable, and faster. In paper [10], the authors specially denoted that the non-surface wave approximation will be efficient to compute the transmission coefficient when the incident angle is small. This paper will also validate this point.

When the non-surface wave approximation is adopted, the transfer matrix \mathbf{T}_i of the i-th unit is a 2×2 matrix: $[T_{11},T_{12};T_{21},T_{22}]$. The total transfer matrix of N-layered media can be accumulated as \mathbf{T}^N , where \mathbf{T}^N is equal to $\mathbf{T}_1\mathbf{T}_2\cdots\mathbf{T}_N$. The incident and transmitted waves can be written as $u(x_1)=e^{iq^{(1)}x_1}+re^{-iq^{(1)}x_1}$ and $u(x_1)=te^{iq^{(1)}x_1}$, with r and t representing the amplitude ratios of the reflected and transmitted plane waves to the incident plane wave, respectively. The state vectors on the incident interface and out-going interface are denoted as $\mathbf{v}_{\rm in}=\{1+r,iq^{(1)}\bar{c}_{44}^{(1)}(1-r)\}^{\rm T}$ and $\mathbf{v}_{\rm out}=e^{iq^{(1)}x_1^{(N)}}\{t,iq^{(1)}\bar{c}_{44}^{(1)}t\}^{\rm T}$, respectively. With the relationship of $\mathbf{v}_{\rm out}$ and $\mathbf{v}_{\rm in}$ with respect to the total transfer matrix $\mathbf{T}^N:\mathbf{v}_{\rm out}=\mathbf{T}^N\mathbf{v}_{\rm in}$, r and t can be solved as

$$r = \frac{T_{21}^{N} + (q^{(1)}\bar{c}_{44}^{(1)})^{2}T_{12}^{N} + iq^{(1)}\bar{c}_{44}^{(1)}[T_{22}^{N} - T_{11}^{N}]}{-T_{21}^{N} + (q^{(1)}\bar{c}_{44}^{(1)})^{2}T_{12}^{N} + iq^{(1)}\bar{c}_{44}^{(1)}[T_{22}^{N} + T_{11}^{N}]}$$

$$t = \frac{i2q^{(1)}\bar{c}_{44}^{(1)}e^{iq^{(1)}x_{1}^{(N)}}}{-T_{21}^{N} + (q^{(1)}\bar{c}_{44}^{(1)})^{2}T_{12}^{N} + iq^{(1)}\bar{c}_{44}^{(1)}[T_{22}^{N} + T_{11}^{N}]}$$
(7)

Table 1Material constants of PZT-4 (sublayer 1) and LiTO₃ (sublayer 2).

Material	Mass density ρ (10 ³ kg/m ³)	Elastic constant c ₄₄ (GPa)	Piezoelectric constant e_{15} (C/m ²)	Dielectric constant ε_{11} (10 ⁻¹¹ F/m)
PZT-4	7.6	25.6	12.7	646
LiTO ₃	3.4	17.8	0.89	6.43

Download English Version:

https://daneshyari.com/en/article/8204806

Download Persian Version:

https://daneshyari.com/article/8204806

<u>Daneshyari.com</u>